Kinematics Characteristics of The Internal & External Geneva Mechanism Under The Effect of Multi Design Parameters

Dr. Nabil N. Swadi
Machines & Equipments Engineering Department, University of Technology/ Baghdad
Email: nabilalbukhturee@yahoo.com

Received on:20/12/2015 & Accepted on:19/5/2016

ABSTRACT:

In this paper, the effect of some design parameters on the kinematic characteristics (displacement, velocity, and acceleration) of the external and internal Geneva Mechanism (GM) has been considered analytically using MATLAB and numerically using Solid Works program. The parameters, such as the change of: the drive pin diameter or the width of slot or the total tolerance, the direction of motion of the pin when it enters or leaves the slot; tangent, above and below to the centerline of the slot, and the number of slots (inside or outside diameter) of the wheel, were taken into account. To compare the results, three, six, and nine slotted external and internal Geneva wheels (GWs) were used for the same crank length and constant driving angular speed. In order to remove the unwanted non-zero initial and final accelerations or jerks, two crank-rocker linkages, the first combining with external six-slot GW and the second combining with internal three-slot GW, were suggested and simulated using SolidWorks program. From that, the angular acceleration of the slotted wheel at the specified (initial and final) positions has been eliminated to zero or reduced to small value. Also, the maximum angular velocity and acceleration of the wheel joining the first linkage has been reduced to about 39.4% and 63.3%, respectively, while in the case of the wheel joining the second linkage, the maximum angular velocity and acceleration has been increased to about 279.4% and 27.4%, respectively.

Keywords: Internal & External GM, SolidWorks, Crank-Rocker linkage

Nomenclature:

d	= pin diameter, (mm)
D_i, D_o	= inside & outside diameter of the internal & external wheel, (mm)
L	= center distance, (mm)
n	= number of slots in driven member (GW)
r	= radius of the driver member, (mm)
R_i, R_o	= inside and outside radius of the GW, (mm)

https://doi.org/10.30684/etj.34.9A.11
2412-0758/University of Technology-Iraq, Baghdad, Iraq

S = length of the slot, (mm)
Tol, TolS= tolerance = (w – d), (mm)
w = width of the slot, (mm)
θ_{o1} = initial angular position of the driver (crank), = 90 (n-2)/ n, (deg.)
θ_{o2} = half angle between the axes of any two successive slots, (deg.)
θ_1, θ_2 = angular position of the driver & GW, (deg.)
ω_1, ω_2 = angular velocity of the driver & GW, (rad/s)
α_2 = angular acceleration of the GW, (rad/s^2)

INTRODUCTION:

The Geneva Mechanism (GM), or some time calls Maltese cross, is a linkage that supplies a discontinuous (intermittent) rotary motion, and it is commonly used in both high and low-rotating speed machines. Generally, GM consists of two important members: the crank with a pin or roller (driver member) and the follower or slotted plate or wheel (driven member) or (GW), see Figure 1.
The crank member provides an intermittent rotation to the follower member and keeps it from spinning between the stages of meeting. The two members should be designed so that the driving pin enters or leaves the slots tangentially. This allows meeting with a lowest amount of impact or shock.

The pin and bearing of the GM should be generously proportioned to carry the large loads regularly encountered.

The driver member typically rotates at a constant angular velocity and when it rotates one revolution, the GW rotates through a small portion of a revolution. This portion of revolution is dependent on the number of slots or stations.

The pins or rollers are frequently made of hardened steel, whereas the GW can be made of steel or cast iron, depending on the powers to be supported. Since the pin is often made of a stiffer metal than the slotted plate, both parts should be taken into account when calculating the load carrying capacity of their two contact surfaces.

The GM is normally used as an indexing device in production machinery. Hence, to keep the GW unmoving and in the appropriate location for the next entry of the pin, the driving member must be built-in with an arc plate (locking plate) which engages an identical cut-out on the boundary of the driven member when the pin is out the slot.
The GM is now widely used in automatic machines, e.g., where an axle or worktable or turret must be indexed. In motion picture projectors, GM is also used to provide the intermittent advance of the film. Moreover, it is widely used in watches and feed mechanisms.

One unwanted feature of the conventional GM is that an acceleration jerk exists at the beginning and ending of the GM motion. Therefore, numerous devices have been suggested to decrease or remove these accelerations jerks. Fenton et al. [1] and Jung [2] improved the motion characteristics of an external GM by transforming the straight radial slots into curved slots GW. Figliolini and Angeles [3] and Figliolini et al. [4] proposed an algorithm on the synthesis of GM drives with curved slots using specified programing motion. Lee and Jan [5] expanded the concept suggested in [4] with highlighting on undercutting. Shigley and Uicker [6] clarified that the slotted curve does reduce the

acceleration, but it increases the deceleration and accordingly the wear on the other side of the slot. In order to eliminate the impact of loading caused by the initial and final acceleration, Barsan [7] considered two approaches; the first one is by replacement the straight slots into curved slots, and the second is by driven the GW using a suitable intermediate cam mechanism. David et al. [8] introduced a non-circular gear pair to regulate the timing of the epitrochoidal path. This method reduces the amount of dangerous jerk to zero value but leads to increase the maximum angular velocity and acceleration of the GW.

In this work, a comparison of the kinematics behavior of an external and internal GM has been presented using both analytical and numerical analysis. For the analytical analysis, the kinematic characteristics (angular displacement, velocity and acceleration) of a GW that contains three, six and nine radial slots are only studied. Whereas for the numerical analysis study, in addition to determine the angular displacement, velocity and acceleration of the GW, the effects of the tolerance (***Tol***) between the pin and slot surfaces, and the angle of tangency above and below the centerline of the slot on the kinematic behaviors are also estimated using the Solid Works software program. Also, this paper presents a simulation of modified crank-rocker mechanisms incorporating with the six-slot External GW and three-slot internal GW to remove the undesirable non-zero initial and final accelerations or jerks (jerk = $d\alpha/dt$) using Solid Works program.

Types of GM*:*

Typically, GM may take three forms: (1) external (most popular); (2) internal (very common) and (3) spherical (generally rare).

This study describes the effects of design parameters on the kinematics behavior for the external and internal GM when the wheel contains three, six, and nine slots.

Analytical Solution:

Kinematics equations for the External GM:

From the six stations (slots) external GM shown in Figure 1, it is obvious that the motion analysis of this mechanism occurs only for 120° ($\theta_{o1} = \pm 60°$) of the rotation of the crank while during the remaining of the rotation angle (240°), the crank is ineffective. Therefore, the active rotation angle of the crank depends on the number of slots that the driven member contains. To avoid the impact between the contact (pin and slot) surfaces, the angle between O_1A and O_2A at the instant of engagement (point A) and disengagement (point A') must be a right angle.

From Figure 1a, using sine law:

$L /sin(90) = r /sin\theta_{o2}$

$\therefore \quad L = r /sin\theta_{o2} = r / sin(180/n)$

Or, $L = a.r$ …(1)

Also, $R_o = \sqrt{L^2 - r^2}$ …(2)

Where, $a = 1/sin (180/n)$; $\theta_{o2} = 360/2n = 180/n$, and n is the number of slots.

From Figure 1b, the motion of the driven member can be analyzed by solving the sides of the triangle into the vertical and horizontal components:

$r \sin\theta_1 = z \sin\theta_2$

Or, $z = r \sin\theta_1 / \sin\theta_2$ …(3)

And, $r \cos\theta_1 + z \cos\theta_2 = L$ …(4)

Eliminate *z* by substituting the equation (3) into (4) gives:

$$\cos\theta_1 + \frac{\sin\theta_1}{\tan\theta_2} = \left(\frac{L}{r}\right) \quad \ldots(5)$$

$$\therefore \quad \tan\theta_2 = \frac{\sin\theta_1}{(a - \cos\theta_1)} \quad \ldots(6)$$

Or, $$\theta_2 = \tan^{-1}\left(\frac{\sin\theta_1}{a-\cos\theta 1}\right) \quad \ldots.(7)$$

Equation (7) represents the angular displacement formula between the crank and star wheel members.

Differentiate Eq. (7) with respect to time to obtain the relation between the angular velocities of the two driver and driven members.

$$(1 + \tan^2\theta_2)\dot{\theta_2} = \frac{a\cos\theta_1 - 1}{(a-\cos\theta_1)^2}\dot{\theta}_1$$

Replacement for $\tan\theta_2$ from Eq. (6) produces, after simplification and reordering:

$$\dot{\theta_2} = \frac{a\cos\theta_1 - 1}{(1+ a^2 - 2a\cos\theta_1)}\dot{\theta}_1 \quad \ldots.(8)$$

Or, $$\omega_2 = \frac{a\cos\theta_1 - 1}{(1+ a^2 - 2a\cos\theta_1)}\omega_1 \quad \ldots(9)$$

Where, $\omega_2 = \dot{\theta}_2 = (d\theta_2/dt)$ *and* $\omega_1 = \dot{\theta}_1 = (d\theta_1/dt)$.

From Eq. (9), it is clear that the maximum GW angular velocity occurs when $\theta_1 = 0$:

$$\omega_{2max} = \frac{a - 1}{(1+ a^2 - 2a)}\omega_1 = \frac{r}{(L-r)}\omega_1 \quad \ldots(10)$$

To describe the relation between the angular accelerations of the driver and follower, Eq. (8) must be again differentiated with respect to time, giving after simplification and regrouping:

$$\ddot{\theta_2} = \frac{a\sin\theta_1(1-a^2)}{(1+ a^2 - 2a\cos\theta_1)^2}\dot{\theta_1^2} + \frac{a\cos\theta_1 - 1}{(1+ a^2 - 2a\cos\theta_1)}\ddot{\theta}_1 \quad \ldots.(11)$$

Usually, the driving member is spinning at constant angular speed. Therefore, the second term of Eq. (11) disappears and it is converted to the following form:

$$\ddot{\theta_2} = \frac{a\sin\theta_1(1-a^2)}{(1+ a^2 - 2a\cos\theta_1)^2}\dot{\theta^2}_1 \quad \ldots(12)$$

Or, $$\alpha_2 = \frac{a\sin\theta_1(1-a^2)}{(1+ a^2 - 2a\cos\theta_1)^2}\omega_1^2 \quad \ldots(13)$$

Where, $\alpha_2 = \ddot{\theta}_2 = d\dot{\theta}_2/dt$

The GW angular acceleration (α_2) reaches its maximum value when:

$$\theta_1 = \pm\cos^{-1}\left\{\sqrt{\left[\frac{1+a^2}{4a}\right]^2 + 2} - \frac{1+a^2}{4a}\right\} \quad \ldots(14)$$

Kinematics equations for the Internal GM:

From the internal GM shown in Figure 2, it is clear that the wheel in this kind of GM rotates in the same direction as the driver, the center distance is less than the wheel radius and the mechanism requires less radial space.

To find the angular displacement, angular velocity and angular acceleration of the driven member of this type of GM, the same foregoing steps will be used:

From Figure 2a, using the law of sine's:

$L /sin (90) = r /sin\theta_{o2}$

$\therefore$ $L = r /sin\theta_{o2} = r / sin (180/n)$

Or, $L = a.r$ …(15)

And, $R_i = \sqrt{L^2 - r^2}$ …(16)

From Figure 2b, solving the sides of the triangle into the vertical and horizontal components yields:

$z \sin\theta_2 = r \sin(180 - \theta_1) = r \sin\theta_1$

Or, $z = r \sin\theta_1 / \sin\theta_2$ …(17)

And, $r \cos (180 - \theta_1) + z \cos\theta_2 = L$ …(18)

Remove *z* by substituting Eq. (16) into (17) gives:

$$-cos\theta_1 + \frac{sin\theta_1}{tan\theta_2} = \left(\frac{L}{r}\right) \quad \text{…(19)}$$

$\therefore$ $$tan\theta_2 = \frac{sin\theta_1}{(a + cos\theta_1)} \quad \text{…(20)}$$

Or, $$\theta_2 = \tan^{-1}\left(\frac{sin\theta_1}{a+cos\theta 1}\right) \quad \text{…(21)}$$

Differentiate Eq. (21) with respect to time to get the relation between the angular speeds of the driver and driven members.

$$(1 + \tan^2\theta_2)\dot{\theta_2} = \frac{a\ cos\theta_1+1}{(a+cos\theta_1)^2}\dot{\theta}_1$$

By replacement for $\tan\theta_2$ from Eq. (20) award, after simplification and reordering:

$$\dot{\theta_2} = \frac{a\ cos\theta_1+1}{(1+ a^2+2a\ cos\theta_1)}\dot{\theta}_1 \quad \text{…(22)}$$

Or $$\omega_2 = \frac{a\ cos\theta_1+1}{(1+ a^2+2a\ cos\theta_1)}\omega_1 \quad \text{…(23)}$$

From Eq. (23), it is clear that the maximum star wheel angular velocity occurs when $\theta_1 = 0$:

$$\omega_{2max} = \frac{a+1}{(1+ a^2+2a\ )}\omega_1 = \frac{1}{(a+1)}\omega_1 = \frac{r}{(L+r)}\omega_1 \quad \text{…(24)}$$

To find the expression between the angular accelerations of the driver and follower, Eq. (20) must be differentiated with respect to time, getting after simplification and rearrangement:

$$\ddot{\theta_2} = \frac{a\ sin\theta_1(1-a^2)}{(1+ a^2+2a\ cos\theta_1)^2}\dot{\theta_1^2} + \frac{a\ cos\theta_1+1}{(1+ a^2+2a\ cos\theta_1)}\ddot{\theta}_1 \quad \text{…(25)}$$

As in previous, the crank is spinning at a constant angular velocity. Therefore, the second term of Eq. (25) vanishes and it is converted to the form below:

$$\ddot{\theta_2} = \frac{a\ sin\theta_1(1-a^2)}{(1+ a^2+2a\ cos\theta_1)^2}\theta_1^2 \quad \text{…(26)}$$

Or, $$\alpha_2 = \frac{a\ sin\theta_1(1-a^2)}{(1+ a^2+2a\ cos\theta_1)^2}\omega_1^2 \quad \text{…(27)}$$

Where, $\alpha_2 = \ddot{\theta_2}$

The maximum α_2 occurs when the pin, in Figure 2, enters (point A) or leaves (point A') the slot, and equals:

$$\alpha_{2max} = \frac{1}{\sqrt{a^2-1}}\omega_1^2 \quad \ldots.(28)$$

Numerical Solution*:*

The 3D model for the GM was created, assembled and motion analyzed using the Solid Works (SW) program [10]. The followings are the important specifications of the GM that have been used for the numerical analysis. The material allocated for the driver, driven and all other members were assumed alloy steel. All driving members used in this work have the crank radius of ***r = 45 mm***, pin diameters (d) depend on the slot width and the amount of tolerance (Tol) proposed. In addition, it is assumed that they rotate with a constant angular speed of $\boldsymbol{\omega_1 = 2\pi}$ ***rad/s (60 rpm)***. Therefore, the total duration time in each case is ***1 second***. Table 1 detailed some additional specifications used for calculating the kinematic characteristics in SW.

In the case of GW associated with a planner crank-rocker linkage, and in order to eliminate or reduce the jerks at the engaged and disengaged points (A and A', see Figures 1a and 1b), a symmetrical coupler curve, which is the locus of a point on the coupler link, and as a consequence, the length of each link in this linkage has been estimated as follows: If the acceleration period may be made equal to the deceleration period, it is useful to make the coupler curve symmetrical. Any symmetrical coupler curve (trace) about an axis may be created by a crank-rocker linkage with a coupler base AB and rocker O_4B of equal length, $AB = O_4B$, Figure 3a, [9]. The coupler point P can generate a symmetrical curve when it lies everywhere on the circle centered at B and passing through A. The above circle must also pass through O_4;

$$AB = O_4B = BP \quad \ldots(29)$$

Therefore, a symmetrical crank-rocker linkage with a well-defined base link L_1 needs only three parameters to describe its geometry. These are L_1/L_2, L_3/L_2, and β because, from Eq. 29, $L_3/L_2 = L_4/L_2 = BP/ L_2$. For given crank length L_2, the final dimensions of the required linkage, that give a symmetrical coupler curve used for 6-slots external GW and 3-slots internal GW, are listed in Table (1) and illustrated in Figures 3b and 4 using SW program.

Slipup (mistake) of GM*:*

In a well-made GM or GW associated with a crank-rocker linkage, the drive or coupler pin will enter in the slots of the wheel along a curve that is tangent to the center line of the slot ($\gamma = 0$), as shown in Figures 1a, 1b, 3b and 4. If the tangent line (direction) of motion of the pin diverges from the slot center line by an angle γ, as shown in Figure 5, a positive or negative impact (i.e., a positive or negative torque on driver member) can result depending on whether the slot is at some angle above ($+\gamma$) or below ($-\gamma$) the tangent line of motion of pin. This situation was also simulated when ($\gamma = \pm 6°$) using SW program for both external and internal GM with three different slotted wheels. The obtained results were plotted and compared in curves.

External Geneva Mechanism						
No. of Slots, n	**θ_{o1}(°)**	**θ_{o2}(°)**	**L, (mm)**	**R_o, (mm)**	**S/ (r+R_o)-L, (mm)**	**w, (mm)**
3	30	60	51.9615	25.9807	19.019	7
6	60	30	90	77.94228	32.94228	11
9	70	20	131.571198	123.636	37.06528	10.5
Internal Geneva Mechanism						
No. of Slots, n	**θ_{o1}(°)**	**θ_{o2}(°)**	**L, (mm)**	**R_i, (mm)**	**S/ (r+L)-R_i, (mm)**	**w, (mm)**
3	30	60	51.9615	25.9807	70.9808	12
6	60	30	90	77.94228	57.05772	12
9	70	20	131.571198	123.636	52.9352	12
External GW associated with a crank-rocker linkage							
No. of Slots, n	**Base (L_1), (mm)**	**Crank (L_2), (mm)**	**Coupler (L_3), (mm)**	**Rocker (L_4), (mm)**	**BP, mm**	**β, (°)**	**w, (mm)**
6	105	35	80	80	80	180	11
Internal GW associated with a crank-rocker linkage							

Table (1): Some design parameters of GM

No. of Slots, n	Base (L_1), (mm)	Crank (L_2), (mm)	Coupler (L_3), (mm)	Rocker (L_4), (mm)	BP, mm	β, (°)	w, (mm)
3	92.112	39.9	80	80	80	180	12

Results and Discussion:

The results can be grouped into two categories as follows: the results for external GM and that for internal GM. For clarity, all results in this work were only plotted through the active period of the driver member (i.e., the dwell period is not shown).

External GM*:*

Figure 6a shows the variation of the angular displacement plots for three-slot GW against the active time of the driver. It is clear that the motion period (active time) is less than the dwell period. This figure represents also the deviation of the angular displacement, carried out by SW, when the tolerance (***Tol***) is ***zero*** and ***1 mm***. The difference was about ***1.18°***, while the active time slightly increased. Figure 6b illustrates the difference in the angular velocity for the mentioned wheel with respect to time. It shows that the magnitude of peak angular velocity occurs when the driver angle is zero. When the ***Tol*** between the pin and slot surfaces is about ***1 mm***, the velocity curve starts at the location delayed about ***0.023 sec.*** from the conventional one (***Tol = 0***), because the pin needs an extra time to contact the slot. At that time, see Figure 6b, the angular velocity of GW is suddenly increased. Likewise, at the position of maximum angular velocity, the pin needs more time, about ***0.0182 sec.***, to slip from one side of the slot to the other. Hence, the angular velocity, after this place, requires dropping sharply to attain the normal condition. Figure 6c represents the distribution of the angular acceleration of the three-slot external GW during driver action period. In addition, this figure shows, for the normal condition, the acceleration plot starts and ends with finite acceleration and deceleration of about ***68.4 rad/s^2***. This means, these non-zero accelerations produce jerk. Due to the ***Tol*** of ***1mm***, an unexpected increase or decrease in the magnitude of the angular acceleration (about ***1760.26 rad/s^2*** and more than ***-3500 rad/s^2***, respectively) has been produced at the instants when the velocity sharply increased and decreased. This leads to create a high impact between the pin and slot sides, which, in turn, generates vibration and noise.

Figure 7 shows the variation of: (a) angular displacement, (b) velocity, and (c) acceleration of the external six-slots GW against the driver action period. The results are obtained from two states: firstly, when there is no mistake, $\gamma = 0°$, and secondly, when the mistake is $\gamma = -6°$. From Figure 7c, it is clear to see that there is a negative impact in the condition when $\gamma = -6°$. This is because the angular velocity, Figure 7b, starts at a certain negative value (about ***– 0.33 rad/s***), and any instantaneous variation in velocity means an infinite acceleration (more than ***-240 rad/s^2***) which, in turn, means shock, vibration, stress, noise, etc.

Figure 8 displays: (a) the angular displacement, (b) velocity, and (c) acceleration curves of the external nine-slots GW versus time that resulted from two conditions:

firstly, when there is no confusion, $\gamma = 0°$, and secondly, when the confusion is $\gamma = +6°$. From Figure 8c, and as a result of the sudden positive change in the angular velocity (about + ***0.32 rad/s,*** Figure 8b), it is evident to find that there is a positive impact (about + ***64.8 rad/s***^{2}) in the condition when $\gamma = +6°$.

Internal GM:

Figure 9a displays the analytical and numerical angular displacement curves for three-slot internal GW against the effective period of the driver motion. This figure represents also the variations of the angular displacement, executed by SW, with ***Tol*** of 0, ***1, and 2 mm***. The difference was ***1.11°*** and ***2.19°*** when the ***Tol*** is ***1*** and ***2 mm***, respectively. The changes in the angular velocity and acceleration for this type of GW, due to ***Tol*** of ***0***, ***1, and 2 mm***, are illustrated in Figures 9b and 9c, respectively. From Figure 9b, when ***Tol*** is about ***2 mm***, the velocity plot starts and increases sharply at the location delayed about ***0.036 sec.*** from that when ***Tol = 0***, because the pin needs an additional time to contact the slot. For this reason, the acceleration at that place jumps to a value more than ***240 rad/s***^{2}, see Figure 9c.

The fluctuations of the kinematic characteristics for 6 and 9-slot internal GW against the driver motion, calculated analytically and numerically, are indicated in Figures 10 and 11, when ***Tol*** is ***0*** and ***0.5 mm*** due to modification in pin diameter or in slot width, respectively. Relatively, and regardless to the number of slots, a similar behavior can be observed in the two figures for each characteristic.

Figures 12 and 13 show the improvement of the kinematic characteristics when the crank-rocker linkage used to drive the 6-slot external and 3-slot internal GW, respectively. It is clear that from these figures, the infinitely jerk (at the initial and final position of engagement) is reduced to zero (see Figure 13) or to small value (see Figure 12). Also, the maximum angular velocity and acceleration of the GW joining the first linkage (case 1) is reduced to about 39.4% and 63.3%, respectively, while in the case of the GW attaching the second linkage (case 2), the maximum angular velocity and acceleration is increased to about 279.4% and 27.4%, respectively.

CONCLUSIONS:

A few overall conclusions can be made about the above results:

1. The results of angular displacement and velocity obtained from the miscellaneous of GM gave a slight difference, whereas in the case of angular acceleration, this miscellaneous produced high impact (depending on the number of slots and initial input angular velocity) when the centerline of the slot was below or above the line tangent to the direction of the pin's motion.
2. In order to eliminate the impact through the period of GW movement, one must reduce as much as possible or eliminate the tolerance (***Tol***) between the pin and slot surfaces.
3. If the 6-slot external GW driven by a crank-rocker linkage instead of a rotary crank, several things achieved. The active period of the wheel is increased. The initial and final accelerations are reduced, not finite, thus reducing the amount of jerk associated with a conventional GM. The peak velocity and acceleration are also decreased.

4. If the 3-slot internal GW driven by a crank-rocker linkage instead of a rotary crank, numerous things occurred. The active period of the wheel is decreased. The initial and final accelerations are eliminated, thus removing the amount of jerk associated with a conventional GM. The peak velocity and acceleration are enlarged.

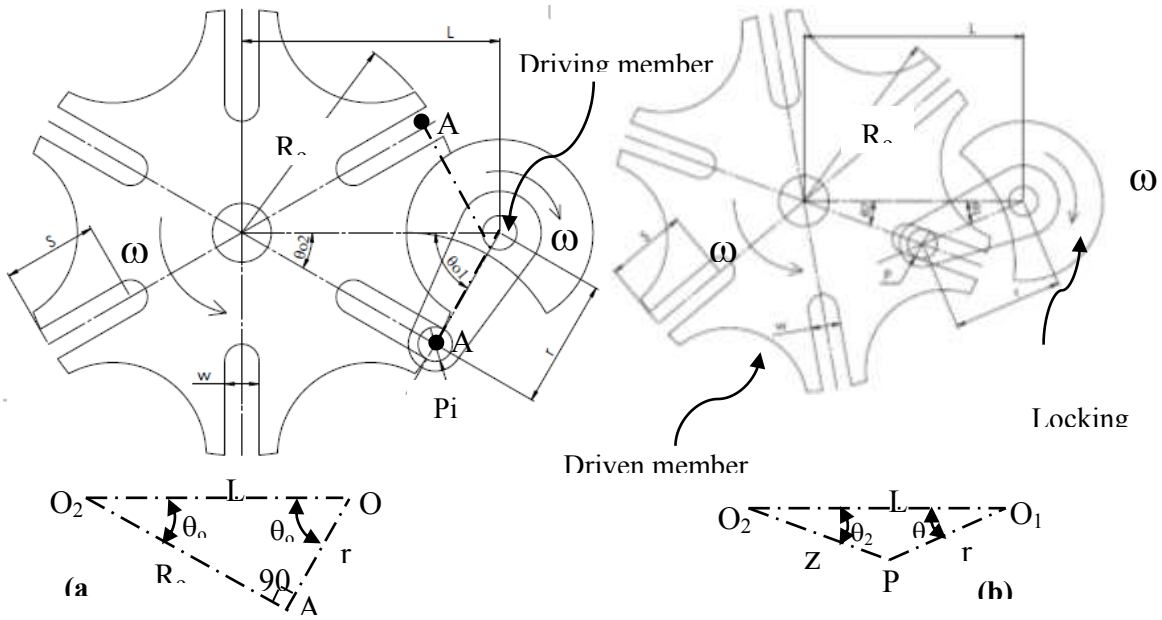

Figure (1): The basic structure of the 6-slot External GM.

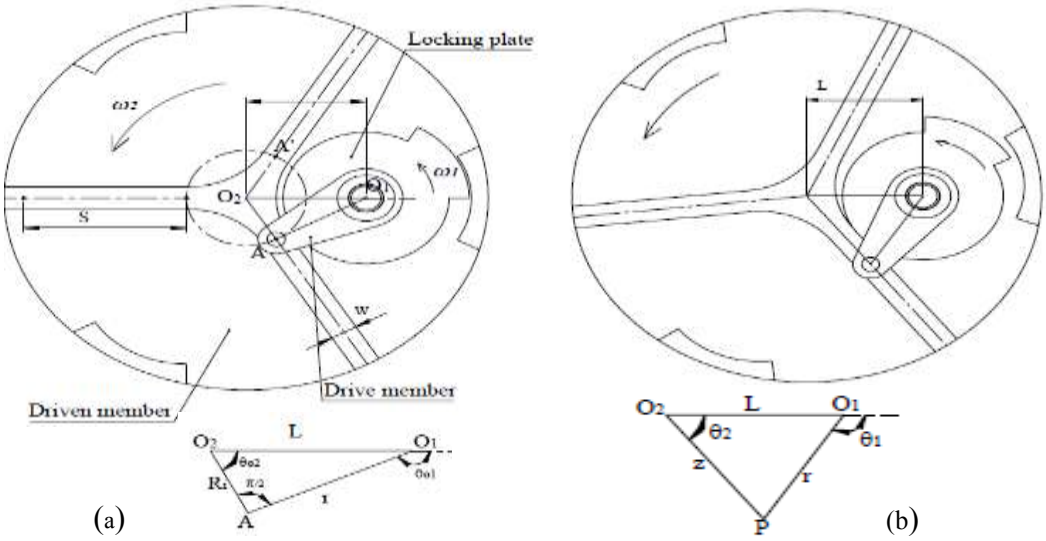

Figure (2): The basic structure of the 3-slot Internal GM.

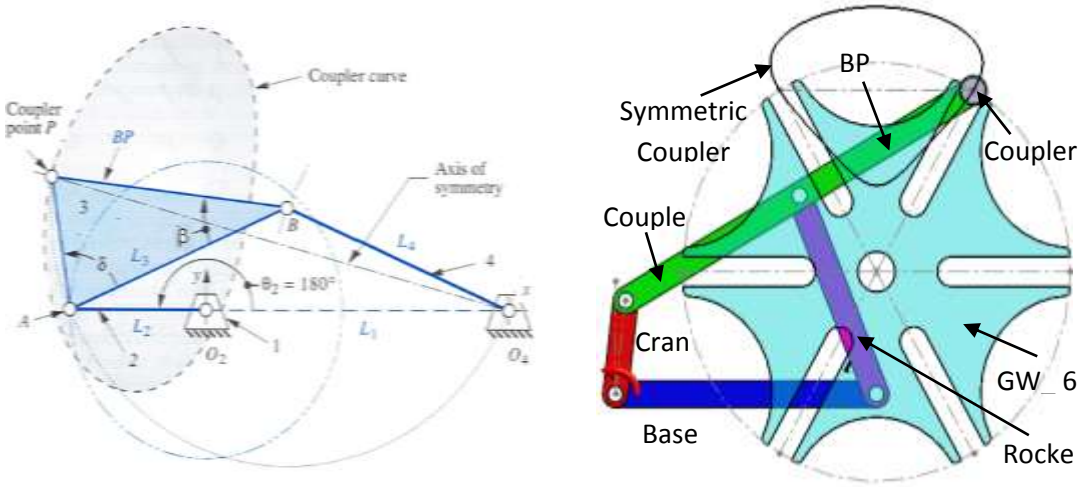

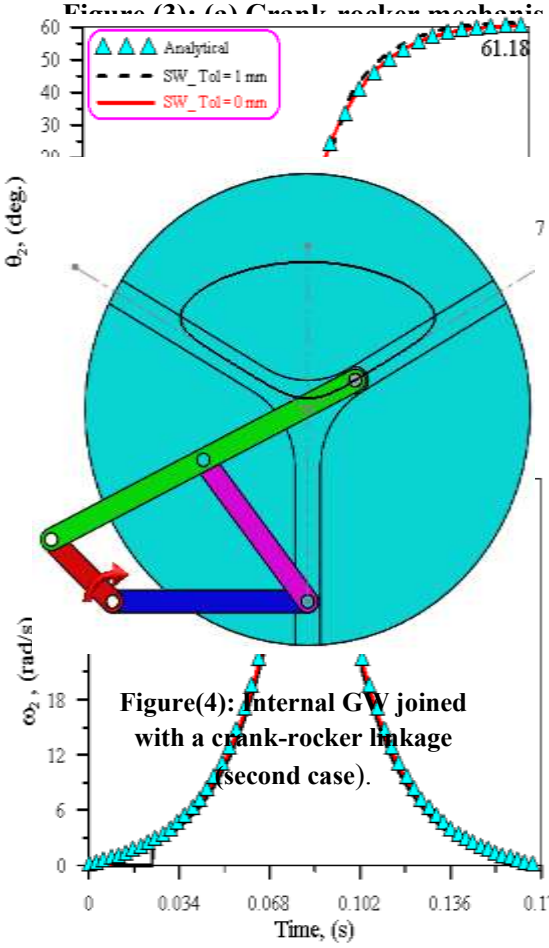

Figure(4): Internal GW joined with a crank-rocker linkage (second case).

(b

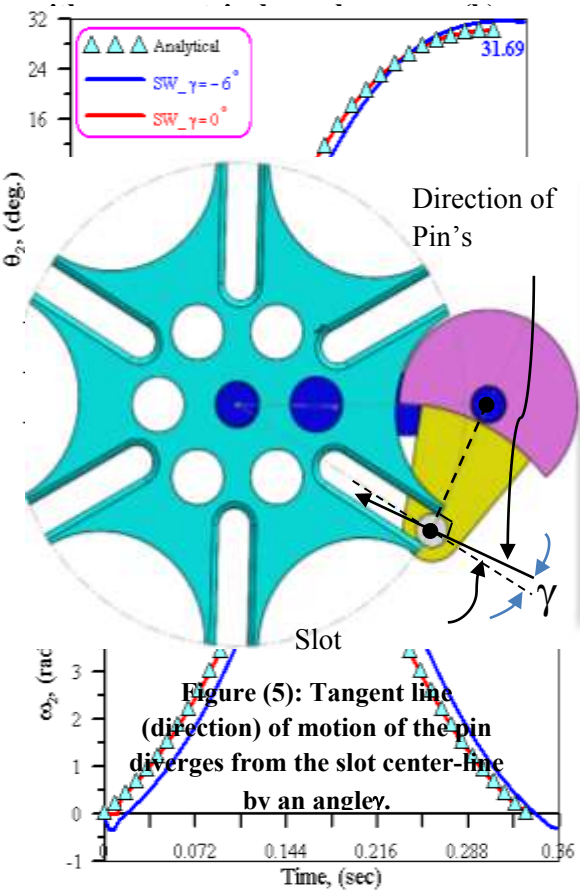

Figure (5): Tangent line (direction) of motion of the pin diverges from the slot center-line by an angle γ.

(b

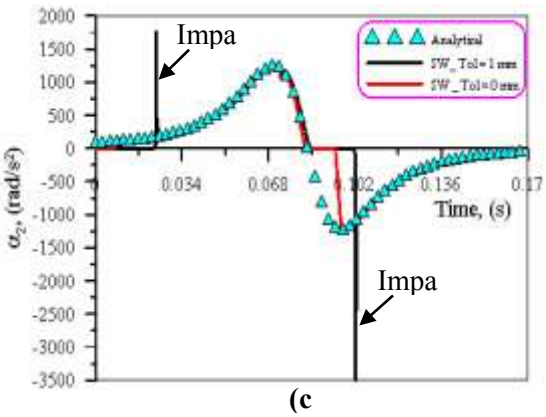

(c

Figure 6: Kinematic characteristics variations for 3-**slot external** GM due to Tol = 0, 1mm.

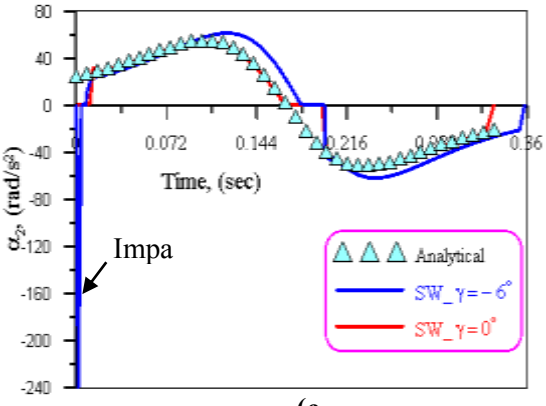

(c

Figure 7: Kinematic characteristics deviations for **6-slot external** GM due to slipup of γ = - 6°.

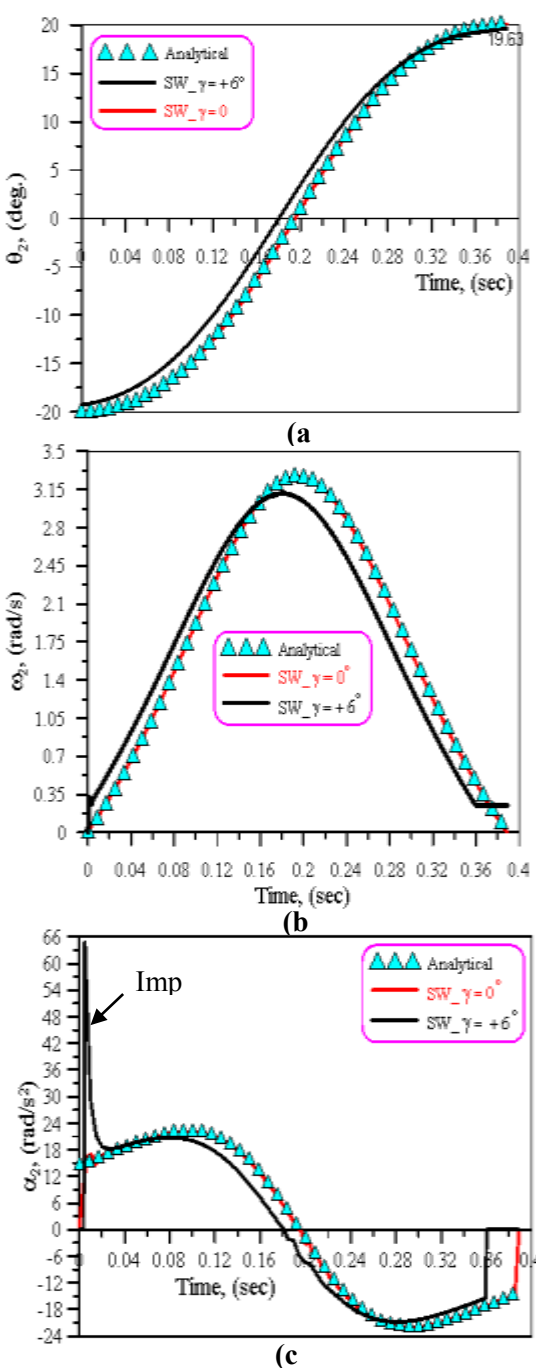

Figure 8: Kinematic characteristics distribution for **9-slot external** GM due to inaccuracy of γ = + 6°.

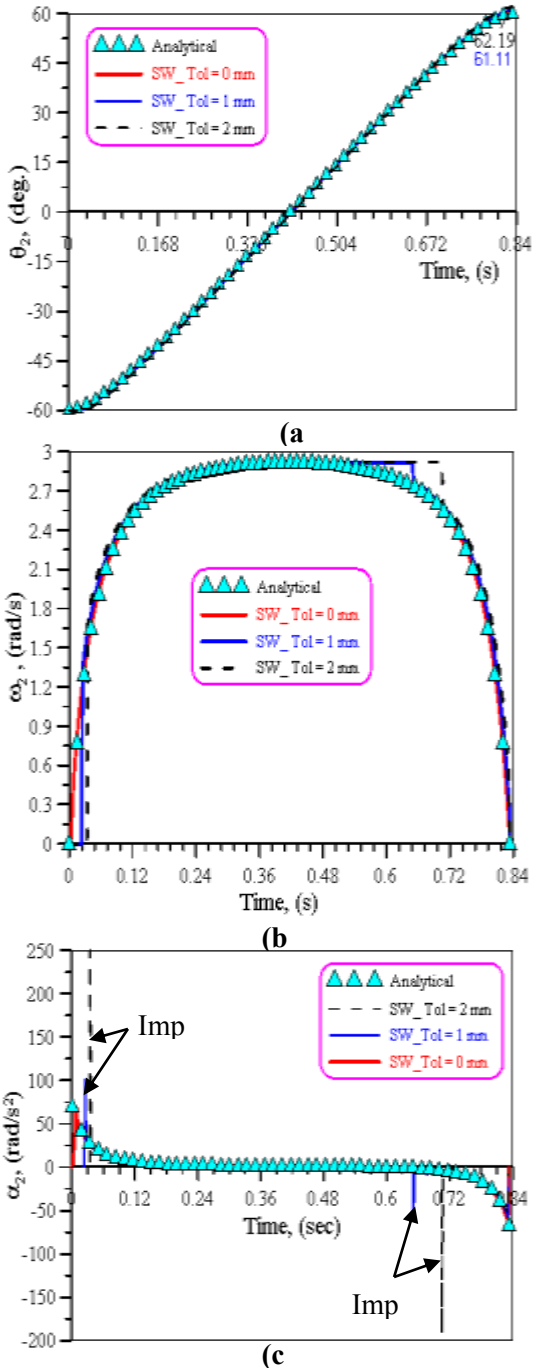

Figure 9: Kinematic characteristics variation for **3-slot internal** GM due to Tol = 0, 1, 2 mm.

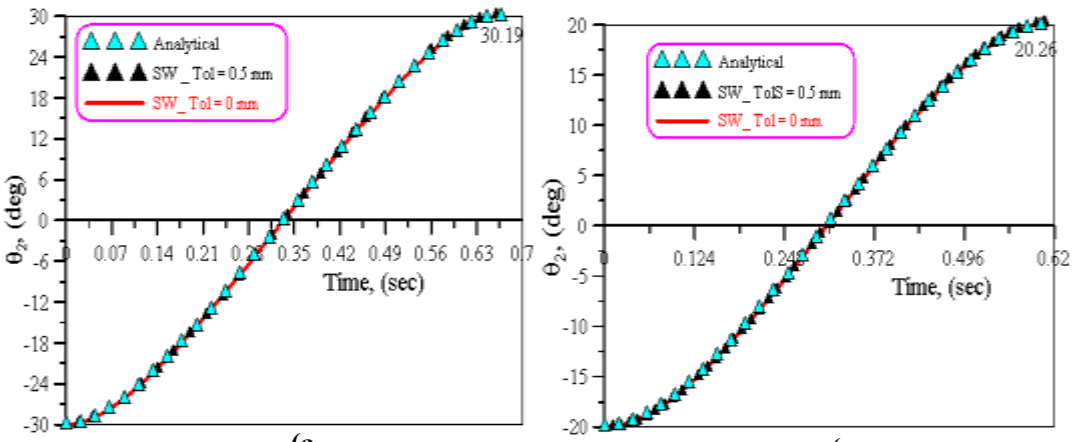
Analytical
SW_Tol=0.5 mm
SW_Tol=0 mm
30.19
θ2, (deg)
Time, (sec)
0.07
0.14
0.21
0.35
0.42
0.49
0.56
0.63
0.7

(a

Analytical
SW_Tol=0.5 mm
SW_Tol=0 mm
20.26
θ2, (deg)
Time, (sec)
0.124
0.248
0.372
0.496
0.62

(a

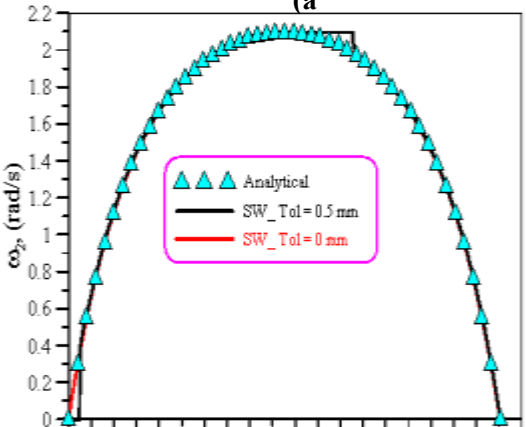
Analytical
SW_Tol=0.5 mm
SW_Tol=0 mm
ω2, (rad/s)

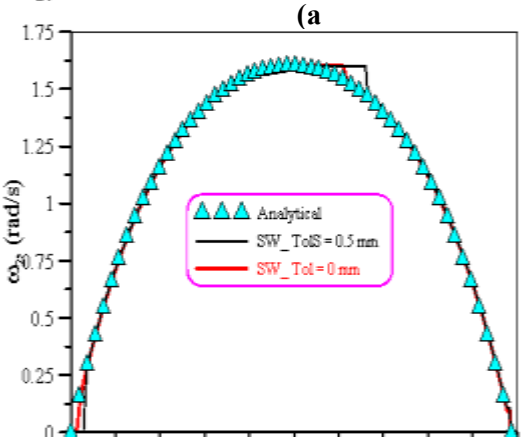
Analytical
SW_Tol=0.5 mm
SW_Tol=0 mm
ω2, (rad/s)

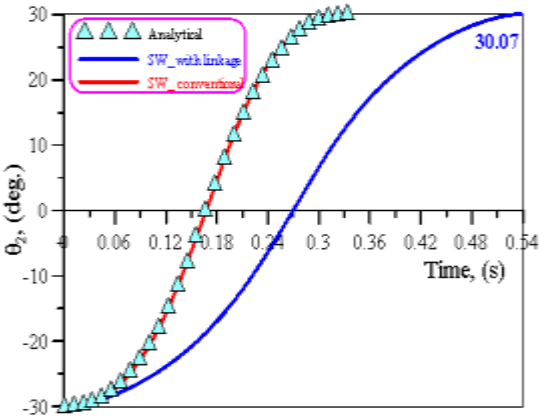

(a)

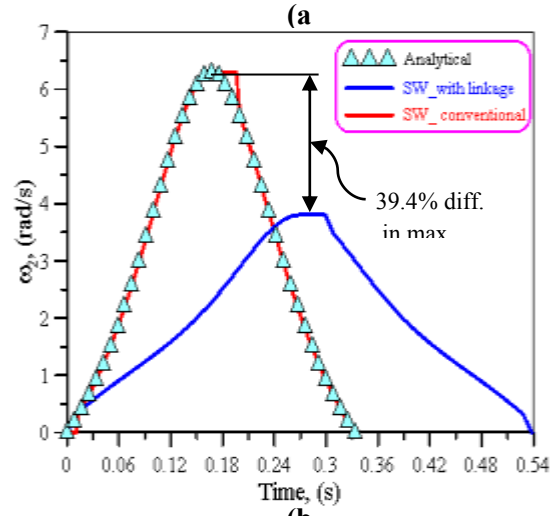

(b)

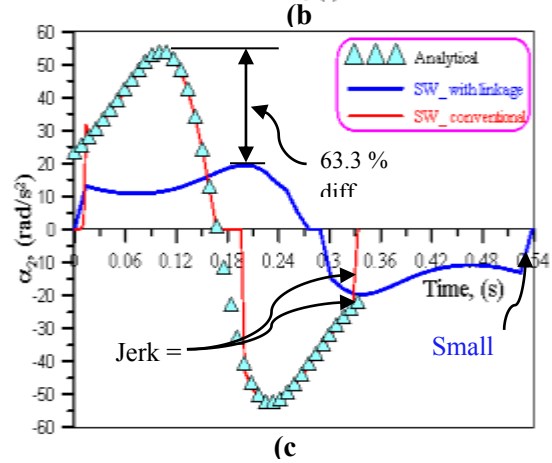

(c)

Figure 12: Curves presenting the movement of a **6-slot external** GW driven by crank-rocker linkage (case 1).

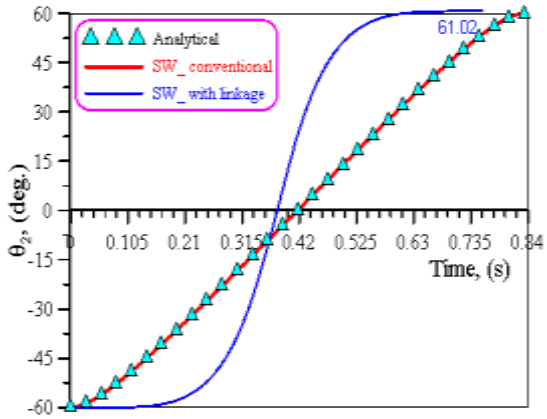

(a)

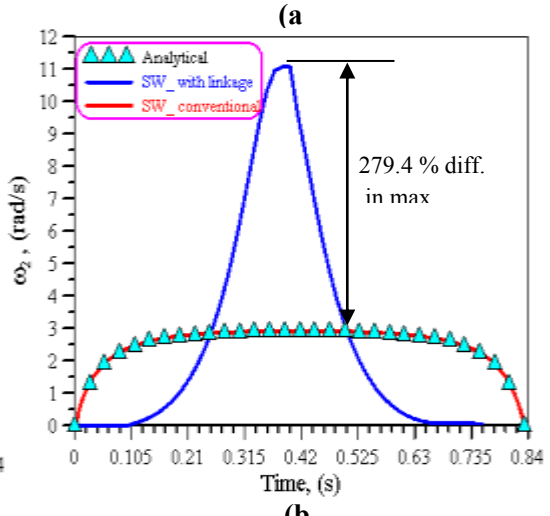

(b)

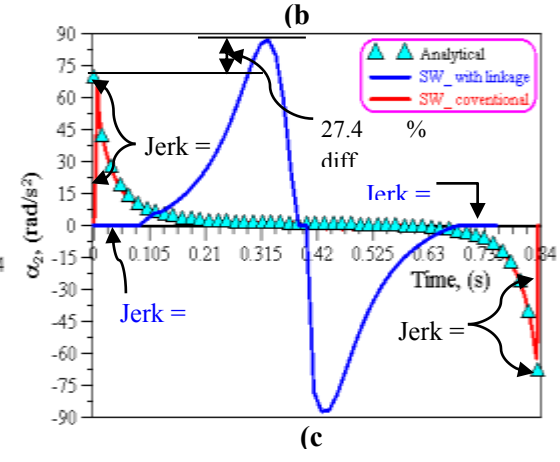

(c)

Figure 13: Curves displaying the movement of a **3-slot internal** GW driven by crank-rocker linkage (case 2).

EFERENCES:

[1].Fenton, R.G., Zhang, Y. & Xu, J., "Development of a new Geneva mechanism with improved kinematic characteristics", ASME Journal of mechanical Design, Vol. 113, pp. 40-45, 1991.

[2].Jung, F.H, "Design and analysis of Geneva mechanism with curved slots", Dep. of Mech. Eng., Far East University, Tainan, Taiwan, 2014.

[3].Figliolini, G. & Angeles, J., "Synthesis of conjugate Geneva mechanism with curved slots", Mechanism and Machine Theory, Vol. 37, pp. 1043-1061, 2002.

[4].Figliolini, G., Rea, P. & Angeles, J.," Synthesis of conjugate Geneva mechanisms and their equivalent Pure-Rolling Cams", 12th IFToMM World Congress, Besançon (France), June 18-21, 2007.

[5].Lee, J.J., & Jan, B.H., "Design of Geneva mechanisms with curved slots for non-undercutting manufacturing", Mechanism and machine Theory, Vol. 44, pp. 1192-1200, 2009.

[6].Shigley, J.E., & Uicker, JR.J.J."Theory of Machines and Mechanisms", McGRAW-HILL, Int. Edition, 1981.

[7].Barsan, A., "Kinematics optimization of the Geneva mechanisms", Journal of technical university of Moldova, Vol. 2, pp. 59-62, 2014.
[8].David, B.D., Antonio, P. and Domenico, M., "An intermittent motion mechanism incorporating a Geneva wheel and a gear train", Canadian Society for Mech. Eng., Vol. 38, No. 3, 2014.
[9].Norton, R.L., "Kinematics and Dynamics of Machinery", 1st Ed., 2009.
[10].SolidWorks User's Manual, Rev. 2015, 2015.